Optimal control based algorithms for energy management of automotive power systems with battery/supercapacitor storage devices

Tran Anh-Tu Nguyen, Jimmy Lauber, Michel Dambrine

Optimal Control Based Algorithms for Energy Management of Automotive Power Systems with Battery/Supercapacitor Storage Devices

Article *in* Energy Conversion and Management · November 2014

DOI: 10.1016/j.enconman.2014.07.042

CITATIONS
74

READS
840

3 authors:

Anh-Tu Nguyen
Université Polytechnique Hauts-de-France
140 PUBLICATIONS **2,084** CITATIONS
SEE PROFILE

Jimmy Lauber
Université Polytechnique Hauts-de-France
154 PUBLICATIONS **2,026** CITATIONS
SEE PROFILE

Michel Dambrine
Université Polytechnique Hauts-de-France
151 PUBLICATIONS **4,316** CITATIONS
SEE PROFILE

Optimal Control Based Algorithms for Energy Management of Automotive Power Systems with Battery/Supercapacitor Storage Devices

AnhTu Nguyen*, Jimmy Lauber, Michel Dambrine

*Corresponding author. Phone +33 (0)3 27 51 14 88. Fax +33 (0)3 27 51 13 16.

The authors are with the LAMIH laboratory UMR CNRS 8201, 59313 Valenciennes Cedex, France.

Email addresses: nguyen.trananhtu@gmail.com; {jimmy.lauber, michel.dambrine}@univ-valenciennes.fr.

***Abstract*—The objective of this work is to show how to control the electric power systems of a vehicle in such a manner that their power flows should be optimized in the sense of energy efficiency. As will be seen, the control problem considered in this work can be formulated as an optimization problem in the presence of several constraints. A systematic approach based on optimal control will be adopted to design the energy management strategies. Then, by means of these strategies, the electric energy will be generated and stored in the most appropriate manner so that the overall energy consumption and eventually the pollutant emissions can be minimized for a given driving cycle. To this end, both non-causal optimization method using the knowledge of the entire driving cycle and causal one are developed for two case studies with different structures of energy storage system. These strategies are then evaluated in an advanced simulation environment to point out their effectiveness.**

***Index Terms*—Energy management system, vehicular electric power system, battery and supercapacitor, Pontryagin's minimum principle, state constraints.**

1. Introduction

Over the years, the demand of electric power consumption in conventional vehicle has become more and more important. This is due to the fact that automotive customers are more and more demanding in terms of performance, comfort and safety for their new vehicles. Hence, the number of auxiliary electric-powered devices has been constantly increased in modern vehicles, e.g. active

suspension, electric brakes, catalyst heaters, etc. This increasing demand tends to double or triple the current vehicle electric load [1]. Besides improving the efficiency of the electric components, an effective energy management strategy (EMS) is also crucial to minimize the overall energy consumption of the vehicle.

In this work, the key feature of the studied vehicle consists in the presence of an electrical supercharger (eSC) in the turbocharged air system of the spark-ignition (SI) engine. This device aims at assisting the main turbocharger to reduce the effects of "turbo lag", i.e. slow engine torque dynamics and lack of torque at low speeds. As a consequent, the drivability is significantly improved. The energy consumption of the eSC is provided by the vehicular electric power system. To this end, the vehicle is equipped with an advanced alternator which is controlled in power. Note that this alternator is directly coupled to the vehicle primary shaft; therefore, the engine operating point can be shifted by controlling the alternator output power. This fact offers one degree of freedom for energy optimization as in the case of classical parallel hybrid electric vehicles. However, this small capacity alternator is exclusively used to generate the energy for the electric power system and cannot assist the internal combustion engine (ICE) to propel the vehicle. Note also that the considered alternator can also recover the kinetic and potential energy during the regenerative braking phases. This "free energy" is then stored in the energy storage system (ESS) and will be used later in appropriate ways.

From the above remarks, it is clear that the energy management becomes very attractive to improve the overall energy efficiency of the studied vehicle. Because of industrial specifications, the developed strategies have to satisfy several objectives. First, they can offer a global optimal solution when the driving conditions are perfectly known in advance, i.e. *offline situations*. Second, their adaptations for real-world driving situations (i.e. *online situations*) are straightforward and the resulting causal strategies behave closely as the global optimal ones. Third, the developed strategies must be simple to be implementable with limited computation and memory resources. Fourth, the strategies are based on a systematic approach so that they can be applicable to a large spectrum of

component dimension without the need for extensive calibration. For all these reasons, the developed EMSs will be based on an optimal control approach using physical component models of the vehicle.

Because of the relevance to this work, a brief overview concerning the optimal based energy management issue for hybrid electric vehicle [2,3] will be provided. In automotive framework, there are mainly two methods based on optimal control theory which may offer a globally optimal result in offline situations: Dynamic Programming (DP) [4] and Pontryagin's Minimum Principle (PMP) [5]. DP-based strategies are known to be very costly in terms of computation. Numerous efforts have been devoted to reduce the computation time [6]. These strategies are often used for offline purposes (performance evaluation, component sizing) [7]. Some adapted online versions can be found in [8,9,10]. Concerning the strategies based on PMP, their optimum could not be global as in the case of DP since the PMP only provides necessary optimality conditions. However, they are much more computationally efficient and the online adaptation is more straightforward. This is the main reason why we only deal with PMP approach in this work. In the literature, many results exist on PMP-based strategies [11,12] or the related Equivalent Consumption Minimization Strategies (ECMS) [13,14]. Besides optimal control based approaches, some rule-based methods for energy management can also be found in literature, see [15,16,17] and references therein.

The main focus of this paper is to propose a systematic approach to design the energy management strategies that optimize the power flow of the vehicular electric power system. To this end, both online and offline strategies are considered. Thank to these optimal based EMSs, the overall energy consumption of the vehicle is minimized under all driving situations. A preliminary study on the choice of the structure of energy storage system was carried out by our industrial partners. From that, two case studies of electric power system with the same vehicle architecture will be considered. These choices are mainly due to the acceptable cost especially for the energy storage devices compared to conventional hybrid vehicles. The first case study is as in a conventional vehicle where only the battery is used to provide all onboard electric consumption and to make the electric

power system more robust against peak-power demands. In this case, the EMS will exploit the freedom that the battery offers to the alternator in deciding the moment to generate electric power. This degree of freedom is generally not used [10]. For the second case study, a hybrid storage system combining a supercapacitor [18] together with a battery will be used. Such a hybrid storage system has been widely used in automotive industry since it has both the high energy density of the battery and the high power density of the supercapacitor [19]. The supercapacitor aims at providing high currents during hard transition phases to protect the battery from fatal damages caused by over-discharge [2]. The supercapacitor is also used to store energy from regenerative braking and to reduce the battery size [19]. As will be seen, battery/supercapacitor hybrid energy storage system is more flexible in terms of optimization than the first one since it offers two degrees of freedom for EMS. However the electric structure and the control design are more complex than the first case.

In this work, we assume that the state constraints concerning the battery are not critical for optimization problem since it can be oversized. However, the supercapacitor may quickly charge and discharge due to its low specific energy compared to the battery [15]. Hence, the state constraints of the supercapacitor should be taken into account. To this end, a new form of penalty function will be proposed by introducing a dummy variable in the expression of the Hamiltonian. The strategies developed in this work are simple to implement, efficient in terms of fuel reduction and of computation times. They can be directly applied to parallel hybrid electric vehicles, and the formulation can be easily generalized to a large family of hybrid vehicles.

The paper is organized as follows. Section 2 first presents the studied vehicle structure with its two different electric power systems. Then, the models of some vehicle components used for control purpose are provided. In Section 3, the optimal control problems are formulated for both case studies and the Pontryagin's Minimum Principle is then applied to design the EMSs. Section 4 is devoted to the implementation issue of the developed EMSs on an advanced dynamic vehicle simulator and the analysis of the obtained results. To this end, the brief description of simulator is first given. Then, a

discussion on how to use the optimal control outputs and also a simple adaptation idea to obtain causal strategies from optimal ones are presented. Next, the simulation results are performed to show the effectiveness of the developed strategies. Finally, a conclusion is given in Section 5.

2. Vehicle Description and Control-Based Models

The considered vehicle architecture is depicted in Figure 1. The notations are given in **Appendix**.

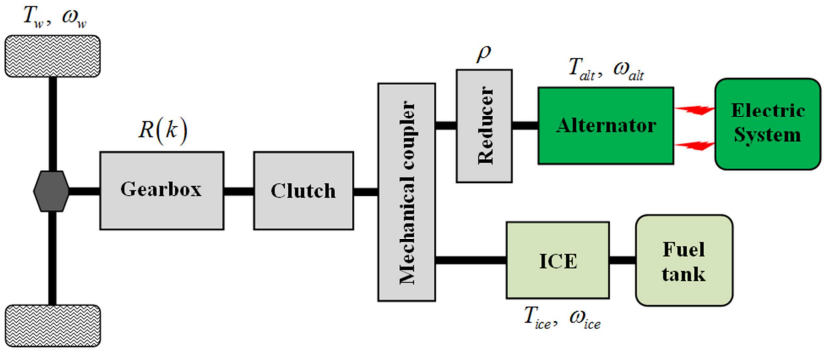

Figure 1. Representation of the studied vehicle architecture

The vehicle is equipped with a conventional powertrain with 5-speed manual transmission. The alternator is connected to the engine with a fixed gear ratio. The only difference between the two considered case studies consists in their electric power system, i.e. the "Electric System" block in Figure 1. The power flow of both case studies is described below.

2.1. Case study 1: Single storage electric power system

The power flow in this case is sketched in Figure 2. The direction of the arrows corresponds to the direction of the energy exchange between different components.

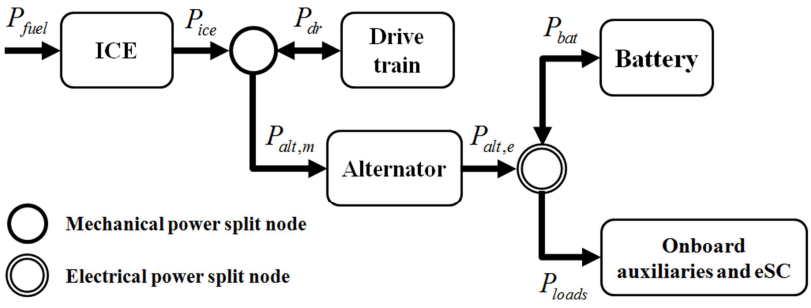

Figure 2. Power flow of the studied vehicle with single storage electric power system

The ICE produces the mechanical power P_{ice} from chemical energy (fuel). This mechanical power P_{ice} is divided into two parts. The first part P_{dr} is used for vehicle propulsion. The second one $P_{alt,m}$ is delivered to the alternator and then converted to electrical power $P_{alt,e}$. The alternator generates the power to satisfy the demand P_{loads} of all onboard auxiliaries including the eSC. It is also used to charge the battery when necessary. The battery power P_{bat} can be negative (when it is charged by the alternator) as well as positive (when it provides electric power for all electrical loads). It should be noticed that the eSC is controlled by engine control unit (ECU) which is out of the present work scope. However, its energy consumption profile is known and will be considered as an input of the developed EMSs.

2.2. Case study 2: Dual storage electric power system

A sketch of the power flow in this case is depicted in Figure 3. It is worth noting that Case study 1 is nothing else than a special case of Case study 2 where the supercapacitor and the DC/DC converter are removed from the electric power system.

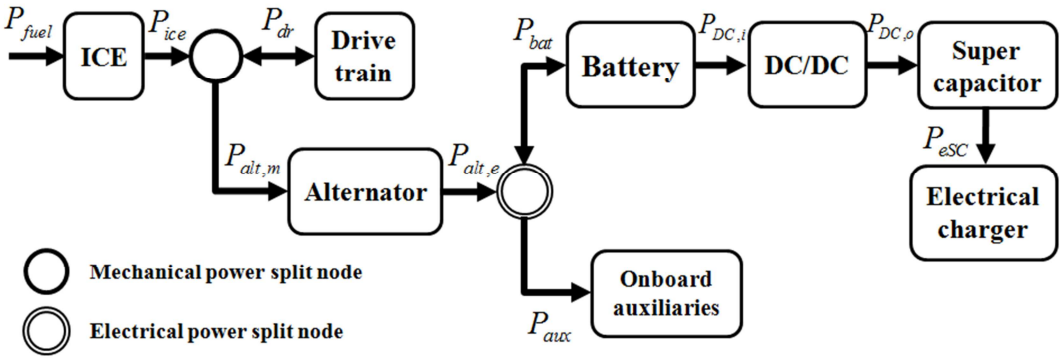

Figure 3. Vehicle power flow in the studied dual storage electric power system

It can be observed that the consumption of onboard auxiliaries P_{aux} can be powered either by the alternator or by the battery. The battery is also used to charge the supercapacitor through the DC/DC converter. However, the supercapacitor cannot charge the battery in this electric structure; it is exclusively used to power the eSC.

2.3. *Vehicle Control-Based Model*

The control models are used to develop the energy optimization algorithm. At each sampling time, the energy optimization algorithm computes the optimal control sequences that minimize the energy consumption of the vehicle. For real-time applications, the control model should have a very limited complexity. Hereafter, some control models of the components of interest for both case studies will be described. It is worth noting that for confidentiality reasons with our industrial partners, all figures showing the data of system components are slightly scaled so that the characteristics of these components will not be revealed.

2.3.1. *Internal combustion engine*

ICE is a complex system where many physical phenomena are not easy to model, e.g. combustion process [20]. However, from an energetic point of view some assumptions can be considered. Here, the temperature dependency and the dynamic behavior of the ICE will be neglected. Then, ICE is characterized by a static look-up-table (LUT) giving the instantaneous fuel consumption in function of the engine torque and the engine speed, see Figure 4.

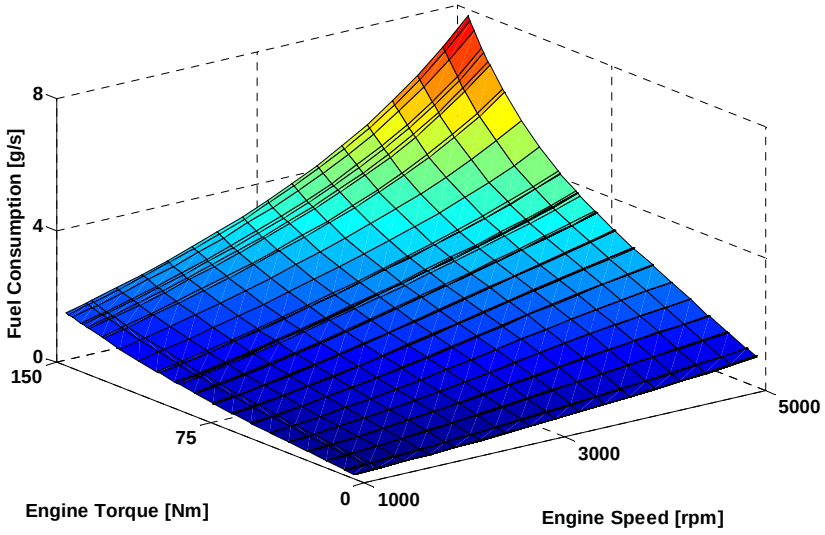

Figure 4. Representation of the instantaneous fuel consumption of the studied engine

Moreover, at a given engine speed, the engine torque is physically limited by its maximum available torque. This characteristic is also represented by a static LUT.

2.3.2. Alternator

The alternator is characterized by some static LUTs as in the case of ICE. The first one, shown in Figure 5, provides the alternator efficiency as a function of the rotary speed and the current. The second LUT needed for the alternator average model provides the maximum current that the alternator can produce as a function of the rotary speed and the current, see Figure 6.

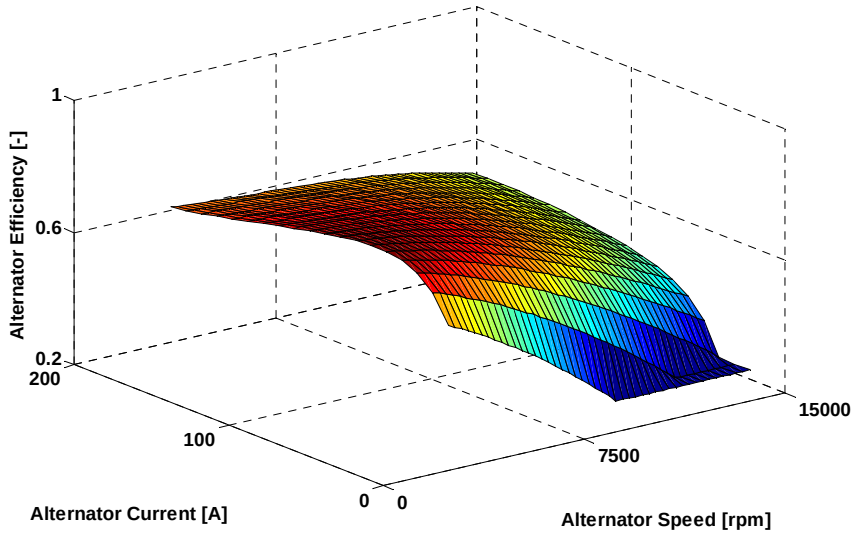

Figure 5. Representation of the alternator efficiency

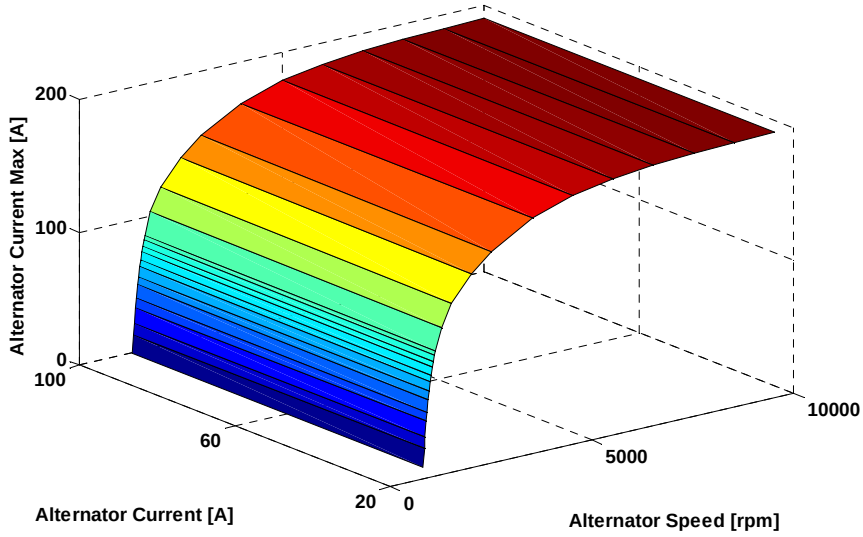

Figure 6. Representation of the alternator maximal current

For energy management strategy design, another LUT providing the maximum available torque at a given alternator speed is also needed. This one guarantees that the alternator torque is always within

its physical limitation. Note that the alternator only works in generator mode, so its current is conventionally positive and is assumed to be measured for the optimization design problem.

2.3.3. Battery

For control purpose, the thermal-temperature effects of the battery are usually neglected. Then, the only state variable left in the battery is its state of charge (SOC) whose dynamics equation is given as follows:

$$\dot{SOC}_{bat}(t) = -\frac{I_{bat}\left(SOC_{bat}(t)\right)}{Q_{bat,0}}; \qquad SOC_{bat}(0) = SOC_{bat,0} \tag{1}$$

where the initial state of charge $SOC_{bat,0}$ and the nominal capacity $Q_{bat,0}$ of the battery are given. The expression of the battery current can be given as [8]:

$$I_{bat}\left(SOC_{bat}(t)\right) = \frac{U_{oc}\left(SOC_{bat}(t)\right) - \sqrt{U_{oc}^2\left(SOC_{bat}(t)\right) - 4R_{bat}\left(SOC_{bat}(t)\right)P_{bat}(t)}}{2R_{bat}\left(SOC_{bat}(t)\right)} \tag{2}$$

where $P_{bat}(t)$ is the battery power at the terminal voltage.

2.3.4. Supercapacitor

After neglecting all complex thermal-electrochemical dynamics, the only state variable left in the supercapacitor is its voltage U_c which is the image of its available energy amount:

$$\dot{U}_c(t) = -\frac{I_{sc}\left(U_c(t)\right)}{C_{sc}}; \qquad U_c(0) = U_{c,0} \tag{3}$$

where the capacitance C_{sc} and the initial voltage $U_{c,0}$ of the supercapacitor are constant and given. Similar to the battery, the supercapacitor current expression can be also given as:

$$I_{sc}\left(U_c(t)\right) = \frac{U_c(t) - \sqrt{U_c^2(t) - 4R_{sc}P_{sc}(t)}}{2R_{sc}} \tag{4}$$

where $P_{sc}(t)$ is the supercapacitor power at the terminal voltage.

2.3.5. DC/DC converter

The DC/DC converter is simply modeled by the following efficiency rate:

$$\eta_{DC} = \frac{P_{DC,o}(t)}{P_{DC,i}(t)} \tag{5}$$

where $P_{DC,o}(t)$ and $P_{DC,i}(t)$ are respectively converter output and input powers. The efficiency of the DC/DC converter is given.

3. Optimal Control Based Energy Management

Hereafter, the optimization problem is formulated for two case studies:

- Case study 1: single storage electric power system
- Case study 2: dual storage electric power system

Next, the PMP will be applied to derive the energy management strategies for these both cases.

3.1. Problem Formulation

3.1.1. Control objective

In this work, the goal of optimal control is to minimize the fuel consumption over the driving cycle in the time optimization horizon $[0,T]$, then the cost function is expressed by:

$$\mathcal{J} = \int_0^T Q_{lhv}\dot{m}_{fuel}\left(T_{ice}(t),\omega_{ice}(t)\right)dt = \int_0^T P_{fuel}\left(T_{ice}(t),\omega_{ice}(t)\right)dt \tag{6}$$

where $P_{fuel}\left(T_{ice}(t),\omega_{ice}(t)\right)$ is the fuel power and the instantaneous fuel consumption of ICE $\dot{m}_{fuel}\left(T_{ice}(t),\omega_{ice}(t)\right)$ is known at a given engine speed ω_{ice} and torque T_{ice}.

Remark 1: The pollutant emissions can be also incorporated by modifying the cost function (6) as:

$$\tilde{\mathcal{J}} = \int_0^T \left(P_{fuel}\left(T_{ice}(t),\omega_{ice}(t)\right) + \sum_{i=1}^{n} \alpha_i \dot{m}_i\left(T_{ice}(t),\omega_{ice}(t)\right) \right) dt \tag{7}$$

where α_i are weighting factors provided by designers and the instantaneous pollutant emission rates $\dot{m}_i\left(T_{ice}(t),\omega_{ice}(t)\right)$ (in general NO_x, CO, HC) are given by static LUTs. However, the objective to

minimize the pollutant emissions is beyond the scope of this paper; therefore only the cost function of the form (6) will be considered in the sequel.

3.1.2. Constraints

a. Vehicle architecture constraints: The mechanical relations between torques and speeds of the considered vehicle architecture represented in Figure 1 are given by the equations:

$$\begin{cases} T_w(t) = R(k(t))\eta_{gb}\left(T_{ice}(t) + \rho T_{alt}(t)\right) = R(k(t))\eta_{gb}T_{ps}(t) \\ \omega_w(t) = \dfrac{\omega_{ice}(t)}{R(k(t))} = \dfrac{\omega_{alt}(t)}{\rho R(k(t))} \end{cases} \quad (8)$$

The driving cycle is usually defined by the couple $(\omega_w(t), k(t))$. Indeed, when $\omega_w(t)$ and $k(t)$ are known, the torque requested at the wheels $T_w(t)$ can be easily derived for the vehicle longitudinal dynamics equation [6]. In this work, engaged gear $k(t)$ at each moment is chosen by the driver. Then, it can be noticed from (8) that, with a given driving cycle, neither the engine speed nor the alternator speed can be chosen by the energy management strategy, the only degree of freedom of the studied architecture is the alternator torque (or ICE torque).

b. Mechanical constraints: Due to the physical limitations of the ICE and the alternator, their speeds and torques are subject to the following constraints:

$$\begin{cases} \omega_{ice,\min} \le \omega_{ice}(t) \le \omega_{ice,\max} \\ \omega_{alt,\min} \le \omega_{alt}(t) \le \omega_{alt,\max} \end{cases} \quad (9)$$

and

$$\begin{cases} T_{ice,\min}\left(\omega_{ice}(t)\right) \le T_{ice}(t) \le T_{ice,\max}\left(\omega_{ice}(t)\right) \\ T_{alt,\min}\left(\omega_{alt}(t)\right) \le T_{alt}(t) \le T_{alt,\max}\left(\omega_{alt}(t)\right) \end{cases} \quad (10)$$

By considering the physical alternator torque limits, the engine torque limits at each instant *t* are given as, where the primary shaft torque $T_{ps}(t) = T_{ice}(t) + \rho T_{alt}(t)$ is derived from the driving cycle:

$$T_{ice}(t) \in \mathcal{T}_{ice} = \left\{ T_{ice}(t) : \underline{T_{ice,\min}}\left(\omega_{ice}(t)\right) \le T_{ice}(t) \le \overline{T_{ice,\max}}\left(\omega_{ice}(t)\right) \right\} \quad (11)$$

where

$$\begin{cases} \underline{T_{ice,\min}}\left(\omega_{ice}(t)\right) = \max\left\{T_{ice,\min}\left(\omega_{ice}(t)\right), T_{ps}(t) - \rho T_{alt,\max}\left(\omega_{alt}(t)\right)\right\} \\ \overline{T_{ice,\max}}\left(\omega_{ice}(t)\right) = \min\left\{T_{ice,\max}\left(\omega_{ice}(t)\right), T_{ps}(t) - \rho T_{alt,\min}\left(\omega_{alt}(t)\right)\right\} \end{cases} \quad (12)$$

c. Electric power system constraints: As mentioned above, the only difference between the two considered case studies consists in their energy storage systems. Case study 1 deals only with one battery, see Figure 7. The optimization problem formulation in this case is similar to the one of conventional parallel hybrid electric vehicles with only one system state of the battery (1).

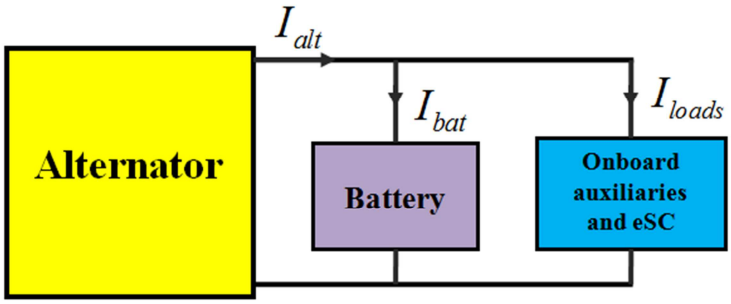

Figure 7. Sketch of the electric structure of Case study 1

From the electric structure in Figure 7, the battery current can be computed as:

$$I_{bat}(t) = I_{alt}(t) - I_{loads}(t) \quad (13)$$

where the electric load current $I_{loads}(t)$ is known and represents all onboard auxiliary demand including the consumption of eSC. The current delivered by the alternator $I_{alt}(t)$ can be easily derived from the optimal alternator torque at each time step. It is noticed from (13) that if the alternator is optimally controlled, then, the battery use is also indirectly optimized in the sense of energy efficiency.

For Case study 2, both battery and supercapacitor are considered. They are linked by a DC/DC converter. The electric structure of this case is depicted in Figure 8. In this case, the dynamics of the supercapacitor (3) should be considered together with (1) for optimization problem to fully take advantage of all electric structure potential.

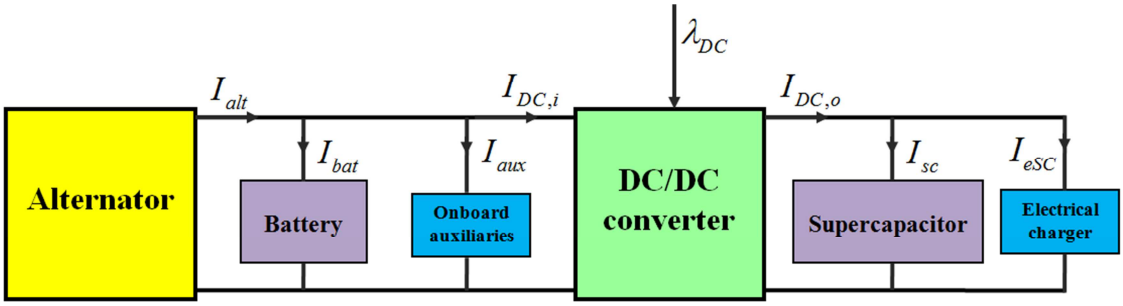

Figure 8. Sketch of the electric structure of Case study 2

In this work, the DC/DC converter controls its output current, i.e. $\lambda_{DC}(t) = I_{DC,o}(t)$. It is noticed that the electric structure of Case study 2 offers a second degree of freedom for optimization problem: the DC/DC output (or input) current. Indeed, if one of these two currents is optimized, the other can be easily deduced from the power relation (5) of DC/DC converter. The battery and supercapacitor currents are respectively computed by the following relations:

$$I_{bat}(t) = I_{alt}(t) - I_{aux}(t) - I_{DC,i}(t) \tag{14}$$

$$I_{sc}(t) = I_{DC,o}(t) - I_{eSC}(t) \tag{15}$$

The DC/DC output current is constrained by:

$$I_{DC,o}(t) \in \mathcal{I}_{DC,o} = \left\{ I_{DC,o}(t) : \underline{I_{DC,o}} \le I_{DC,o}(t) \le \overline{I_{DC,o}} \right\} \tag{16}$$

where $\underline{I_{DC,o}}$ and $\overline{I_{DC,o}}$ are respectively the minimum and maximum output current of the converter.

For safe operation and cycle life extension, the battery SOC and battery current are both limited:

$$SOC_{bat,\min} \le SOC_{bat}(t) \le SOC_{bat,\max} \tag{17}$$

$$I_{bat,\min} \le I_{bat}(t) \le I_{bat,\max} \tag{18}$$

For the supercapacitor, the voltage U_c and the current I_{sc} are subject to the following constraints:

$$U_{c,\min} \le U_c(t) \le U_{c,\max} \tag{19}$$

$$I_{sc,\min} \le I_{sc}(t) \le I_{sc,\max} \tag{20}$$

Both battery and supercapacitor are considered as energy buffer systems. Therefore, the *charge sustaining condition* should be fulfilled by EMS for both of them. Concretely, one should have $\Delta SOC_{bat} \approx 0$ and $\Delta U_c \approx 0$ where:

$$\Delta SOC_{bat} \triangleq SOC_{bat}(T) - SOC_{bat}(0) \tag{21}$$

$$\Delta U_c \triangleq U_c(T) - U_c(0) \tag{22}$$

3.2. Application of Pontryagin's Minimum Principle

Next, the PMP will be applied to the two cases. Only offline optimal solutions will be considered in this subsection. Thereafter, for simplicity, the explicit time-dependence of the variables is omitted except for confusing situations.

3.2.1. Case study 1: Single storage electric power system

Taking into account (1) and (6), the Hamiltonian in this case is defined as:

$$\mathcal{H}(SOC_{bat}, T_{ice}, \lambda_1) = P_{fuel}(T_{ice}, \omega_{ice}) - \lambda_1 \frac{I_{bat}(SOC_{bat})}{Q_{bat,0}} \tag{23}$$

where the battery current $I_{bat}(SOC_{bat})$ is computed by (13). The necessary optimality conditions provided by PMP in this case are given as:

$$\dot{SOC}^*_{bat} = \frac{\partial \mathcal{H}(\cdot)}{\partial \lambda_1} = -\frac{I_{bat}(SOC^*_{bat})}{Q_{bat,0}}; \quad SOC^*_{bat}(0) = SOC_{bat,0} \tag{24}$$

$$\dot{\lambda}^*_1 = -\frac{\partial \mathcal{H}(\cdot)}{\partial SOC_{bat}} = \frac{\lambda^*_1}{Q_{bat,0}} \frac{\partial I_{bat}(SOC^*_{bat})}{\partial SOC_{bat}} \tag{25}$$

$$SOC^*_{bat}(T) \approx SOC_{bat,0} \tag{26}$$

$$SOC_{bat,\min} \le SOC^*_{bat} \le SOC_{bat,\max} \tag{27}$$

$$\mathcal{H}(SOC^*_{bat}, T^*_{ice}, \lambda^*_1) \le \mathcal{H}(SOC^*_{bat}, T_{ice}, \lambda^*_1); \quad \forall t \in [0,T]; \quad \forall T_{ice} \in \mathcal{T}_{ice} \tag{28}$$

Several comments can be made regarding these optimality conditions. First, the conditions (24) and (25) provide respectively the dynamics of the system state and its associated co-state. However,

neither an initial condition nor a final condition on the co-state is available. Second, it is important to emphasize that when the charge sustaining condition guaranteed by (26) is required for the EMS, the battery usually operates only in a small range of SOC [21]. As a consequence, the open circuit voltage and the internal resistance of the battery may not vary so much in this range. Therefore, from (2), it can be concluded that the battery current $I_{bat}\left(SOC_{bat}\right)$ is not significantly affected by the variation of battery SOC. Combining this fact with condition (25), it follows that:

$$\dot{\lambda}_1 \approx 0 \quad \Rightarrow \quad \lambda_1 = \lambda_{10} \tag{29}$$

where the constant λ_{10} has to be determined. This assumption has been exploited in many other previous works [11,6,21]. Third, our studied battery has an important nominal capacity $Q_{bat,0}$, then, the state constraints (27) will never be violated. Fourth, at each instant t, the optimal control T_{ice}^{*} minimizing the Hamiltonian can be exhaustively searched in the torque admissible set $\mathcal{T}_{ice}$ defined in (11). This can be numerically done by testing all torque possibilities of the set $\mathcal{T}_{ice}$ at each time step. Hence, the constraints on the control variable T_{ice} are "naturally" considered. Fifth, it is clear that the optimal solution at each instant t depends on the initial conditions of the system state $SOC_{bat,0}$ and the co-state λ_{10}. The former initial condition is given, however, the latter on is not known *a priori*. The value of λ_{10} depends on boundary condition of the terminal cost at final time T, i.e. the future information of the driving conditions. Indeed, the determination/estimation of this value is crucial to reach the optimal solution as close as possible. For offline situations where driving cycles are given in advance, the value of λ_{10} can be iteratively computed by a "root finding algorithm" [11].

3.2.2. Case study 2: Dual storage electric power system

In this case, two dynamical systems (1) and (3) are available for the energy storage system. As previously highlighted, the state constraints (19) of the supercapacitor should be taken into account. To this end, a new dummy variable has been introduced whose dynamics is defined as [22]:

309 $$\dot{X}_d \triangleq T\left(U_c\right) \tag{30}$$

310 where the function $T\left(U_c\right)$ in (30) is defined as:

311 $$T\left(U_c\right) = \left[U_c - U_{c,\min}\right]^2 sg\left(U_{c,\min} - U_c\right) + \left[U_{c,\max} - U_c\right]^2 sg\left(U_c - U_{c,\max}\right) \tag{31}$$

312 and the function $sg\left(\cdot\right)$ in (31) is given as:

313 $$sg\left(x\right) \triangleq \begin{cases} 0, & x < 0 \\ 1, & x \geq 0 \end{cases} \tag{32}$$

314 Note that $\dot{X}_d\left(t\right) \geq 0,\ \forall t \in \left[0,T\right]$ and $\dot{X}_d\left(t\right) = 0$ only for times when the state constraints (19) are

315 satisfied. The new dummy variable $X_d\left(t\right)$:

316 $$X_d\left(t\right) = \int_0^t \dot{X}_d\left(t\right) dt + X_d\left(0\right) \tag{33}$$

317 is required to satisfy the two boundary conditions: $X_d\left(0\right) = 0$ and $X_d\left(T\right) = 0$. This fact implies once

318 again that $X_d\left(t\right) = 0,\ \forall t \in \left[0,T\right]$. However, it is possible only if the state constraints (19) are

319 satisfied for all $t \in \left[0,T\right]$.

320 Taking into account the dynamics (1), (3) and (30), the augmented Hamiltonian for the Case study 2

321 is defined as follows:

322 $$\begin{aligned} \mathcal{H}_a\left(SOC_{bat}, U_c, T_{ice}, I_{DC,o}, \lambda_1, \lambda_2\right) = P_{fuel}\left(T_{ice}, \omega_{ice}\right) - \lambda_1 \frac{I_{bat}\left(SOC_{bat}\right)}{Q_{bat,0}} \ \cdots \\ - \lambda_2 \frac{I_{sc}\left(U_c, I_{DC,o}\right)}{C_{sc}} + \lambda_d T\left(U_c\right) \end{aligned} \tag{34}$$

323 Then, the necessary optimality conditions are given by (24)-(27) together with the following ones:

324 $$\dot{U}_c^* = \frac{\partial \mathcal{H}_a\left(\cdot\right)}{\partial \lambda_2} = -\frac{I_{sc}\left(U_c^*, I_{DC,o}^*\right)}{C_{sc}}; \quad U_c^*\left(0\right) = U_{c,0} \tag{35}$$

325 $$U_c^*\left(T\right) \approx U_{c,0} \tag{36}$$

326 $$U_{c,\min} \leq U_c^* \leq U_{c,\max} \tag{37}$$

$$\begin{aligned}\dot{X}_d^* &= \frac{\partial \mathcal{H}_a(\cdot)}{\partial \lambda_d} = \left[U_c^* - U_{c,\min}\right]^2 sg\left(U_{c,\min} - U_c^*\right) + \left[U_{c,\max} - U_c^*\right]^2 sg\left(U_c^* - U_{c,\max}\right) \\ X_d^*(0) &= 0\end{aligned} \tag{38}$$

$$\begin{aligned}\dot{\lambda}_2^* = -\frac{\partial \mathcal{H}_a(\cdot)}{\partial U_c} = \frac{\lambda_1^*}{Q_{bat,0}} \frac{\partial I_{bat}\left(SOC_{bat}^*\right)}{\partial U_c} + \frac{\lambda_2^*}{C_{sc}} \frac{\partial I_{sc}\left(U_c^*, I_{DC,o}^*\right)}{\partial U_c} \ \cdots \\ -2\lambda_d^*\left[U_c^* - U_{c,\min}\right] sg\left(U_{c,\min} - U_c^*\right) - 2\lambda_d^*\left[U_{c,\max} - U_c^*\right] sg\left(U_c^* - U_{c,\max}\right)\end{aligned} \tag{39}$$

$$\dot{\lambda}_d^* = -\frac{\partial \mathcal{H}_a(\cdot)}{\partial X_d} \tag{40}$$

$$\begin{aligned}&\mathcal{H}_a\left(SOC_{bat}^*, U_c^*, T_{ice}^*, I_{DC,o}^*, \lambda_1^*, \lambda_2^*, \lambda_d^*\right) \le \mathcal{H}_a\left(SOC_{bat}^*, U_c^*, T_{ice}, I_{DC,o}, \lambda_1^*, \lambda_2^*, \lambda_d^*\right); \\ &\quad \forall t \in [0,T]; \quad \forall \left(T_{ice}, I_{DC,o}\right) \in \mathcal{T}_{ice} \times \mathcal{I}_{DC,o}\end{aligned} \tag{41}$$

As in Case study 1, $\lambda_1 = \lambda_{10}$, $\forall t \in [0,T]$ and at each instant t, the optimal control inputs $T_{ice}^*(t)$ and $I_{DC,o}^*(t)$ minimizing the Hamiltonian can be exhaustively searched in the torque and current admissible sets $\mathcal{T}_{ice}$ and $\mathcal{I}_{DC,o}$ defined respectively in (11) and (16).

Since X_d does not appear explicitly in $\mathcal{H}_a(\cdot)$, then, it can be deduced from (40) that:

$$\dot{\lambda}_d^* = -\frac{\partial \mathcal{H}_a(\cdot)}{\partial X_d} = 0 \quad \Rightarrow \quad \lambda_d^* = \lambda_{d0} \tag{42}$$

where λ_{d0} is the constant to be determined. Note that if the supercapacitor has an important capacitance C_{sc}, its state constraints (19) will be then trivial. In this case, λ_{d0} can be set equal to 0, which means that the supercapacitor state constraints are not taken into account.

From the supercapacitor current $I_{sc}(U_c)$ expression in (4), it follows that:

$$\frac{\partial I_{sc}(U_c)}{\partial U_c} = -\frac{I_{sc}(U_c)}{\sqrt{U_c^2 - 4R_{sc}P_{sc}}} \tag{43}$$

Then, the condition (39) can be rewritten as:

$$\dot{\lambda}_2^* = \frac{-\lambda_2^* I_{sc}\left(U_c^*\right)}{C_{sc}\sqrt{\left(U_c^*\right)^2 - 4R_{sc}P_{sc}}} \cdots$$
$$-2\lambda_{d0}\left[U_c^* - U_{c,\min}\right] sg\left(U_{c,\min} - U_c^*\right) - 2\lambda_{d0}\left[U_{c,\max} - U_c^*\right] sg\left(U_c^* - U_{c,\max}\right) \quad (44)$$

The trajectory λ_2^* is obtained by integrating both sides of (44) which $\lambda_2^*(0) = \lambda_{20}$ has to be determined.

The optimization problem of Case study 2 is now reduced to the choice of the three values λ_{10}, λ_{20} and λ_{d0} in such a manner that both boundary conditions (charge sustaining conditions) (26) and (36) are satisfied. However, using a "root finding algorithm" as in Case study 1 to iteratively compute these three values would not be appropriate due to excessive computation times. A simple method, which is more effective in terms of computation times, will be proposed latter. Although this method only offers sub-optimal control sequences of T_{ice}^* and $I_{DC,o}^*$, it can be directly used for online implementation.

3.2.3. Physical interpretation of Hamiltonian

This subsection aims at pointing out the physical meaning of the Hamiltonians and the co-states in the previous definitions (23) and (34). To this end, only Hamiltonian of Case study 2 is considered since it is of a more general form than the one in (23).

Let us define the following variables:

$$s_1 \triangleq -\frac{\lambda_1}{U_{oc}\left(SOC_{bat}\right)Q_{bat,0}}; \quad s_2 \triangleq -\frac{\lambda_2}{U_c C_{sc}} \quad (45)$$

Then, the expression of the Hamiltonian in (34) can be rewritten as:

$$\mathcal{H}_a\left(SOC_{bat}, U_c, T_{ice}, I_{DC,o}, s_1, s_2\right) = P_{fuel}\left(T_{ice}, \omega_{ice}\right) + s_1 P_{bat,i}\left(SOC_{bat}\right) \cdots$$
$$+ s_2 P_{sc,i}\left(U_c, I_{DC,o}\right) + \lambda_d T\left(U_c\right) \quad (46)$$

where $P_{fuel}\left(T_{ice}, \omega_{ice}\right)$, $P_{bat,i}\left(SOC_{bat}\right)$ and $P_{sc,i}\left(U_c, I_{DC,o}\right)$ are respectively the fuel power, the inner battery power and the inner supercapacitor power. The physical meaning of the Hamiltonian becomes

clearer with (46). Indeed, this is the sum of the weighted powers of all energy sources available in the vehicle. In other words, the Hamiltonian represents an *equivalent fuel power*; and the variables s_1 and s_2 are used to converts the inner battery power and the inner supercapacitor power into the equivalent quantities of fuel power. That is why these variables are usually referred to *equivalence factors* [13,14]. The more important these variables are, the more expensive the electric energy is. So, it is more beneficial to recover the energy by regenerative braking. On the contrary, the lower these variables are, the cheaper the electric energy is also. As a consequent, it is more beneficial to use the electric machine to generate the energy (for the case of hybrid vehicles).

In the cases where the state constraints are present, the dynamics $\dot{X}_d$ indicates these constraints are whether or not violated. Then, the term $\lambda_d \dot{X}_d = \lambda_{d0} \dot{X}_d$ is incorporated into the Hamiltonian as a penalty function. The constant λ_{d0} should be selected to be very high such that the supercapacitor state lies in its bound limits in very short time. Since there is no penalty if the state remains between its upper and lower limits, the energy management strategies can make full use of the supercapacitor over the allowable range.

4. Implementation and Results Analysis

4.1. Dynamic Vehicle Simulator

Before analyzing the results, it should be noticed that all developed strategies in this work are validated with a dynamic vehicle simulator calibrated with real vehicle data. This simulator consists of all appropriate models of different elements constituting the studied vehicle, including the driver and the energy management strategy. An overview of the simulation environment in this work is illustrated in Figure 9. As can be seen, the considered simulation environment has two separated parts: the vehicle model part and the energy management system part.

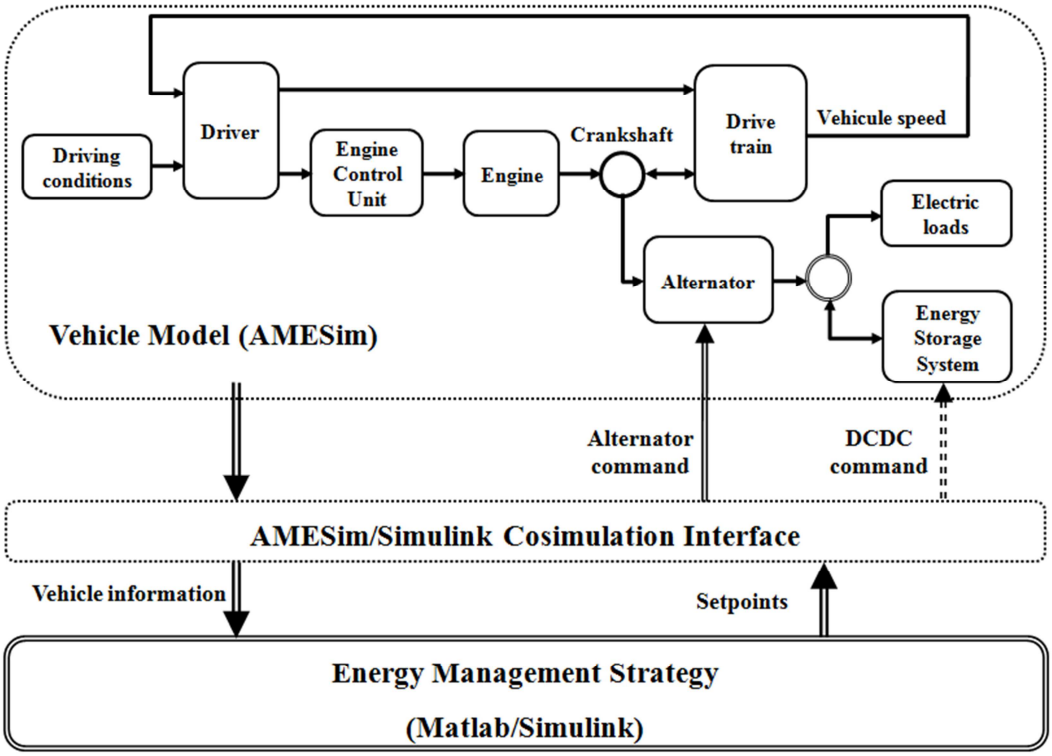

Figure 9. Simulation environment in the thesis framework

The energy management system part is our optimization algorithm coded in **C**-language for time computation efficiency and implemented in Matlab/Simulink as an S-function. The vehicle model part accurately represents all relevant characteristics of the real vehicle. This one is implemented in LMS Imagine.Lab AMESim platform which is inspired by Bond Graph approach [23]. The model and control strategies involved of this dynamic vehicle simulator have been developed by our industrial partners and will not be exposed here for confidentiality. The two parts of the simulation environment are interconnected by a co-simulation interface. The most advantage of this simulation approach is that it offers at the same time the realistic vehicle model and the great convenience of Matlab/Simulink in terms of control design.

In what follows, some issues directly related to the implementation of the developed energy management strategies into the simulator are first discussed. Next, a simple idea to derive a causal EMS for real-time applications is presented. Then, to show the performance of the developed strategies in terms of energy consumption efficiency, they will be also compared to a baseline

strategy where the energy storage system (ESS: battery and/or supercapacitor) will be practically never charged or discharged. As a consequent, the alternator will be always activated to generate all energy needed for onboard electric demand. Note also that these baseline strategies, provided by our industrial partners, will not be detailed for confidentiality reason.

4.2. Implementation

4.2.1. How to use the optimal control sequences?

The developed EMSs provide the engine torque and also the alternator torque in both case studies. They are often used as reference signals to control the ICE and the alternator, respectively. However, in this project, the ECU is designed by another industrial partner and only optimal alternator torque T_{alt}^{*} will be used to control the reference voltage of the alternator. The control scheme of the alternator is illustrated in Figure 10.

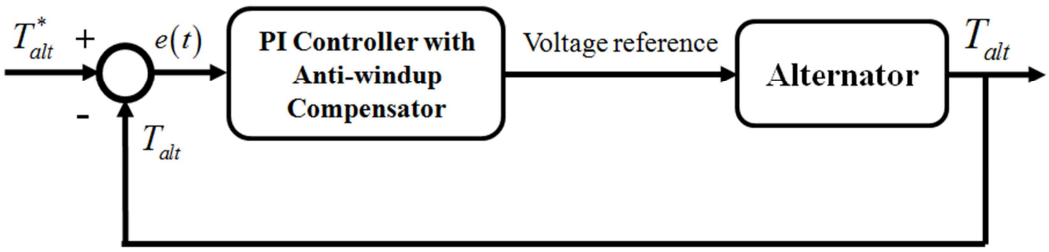

Figure 10. Control scheme of the alternator

For Case study 2, the EMS provides also the optimal control sequence $I_{DC,o}^{*}$ which will be used to control the DC/DC converter as shown in Figure 8.

It is important to remark that the approach used in our work does not require any modifications of the vehicle structure (drive train and electric power system). The only simple task for implementation is to replace the existing controller(s) of the baseline strategy with those developed in this paper.

4.2.2. Online adaptation

As previously emphasized, it is possible to obtain the optimal solutions only when all information of the entire driving cycle is available *a priori*. In subsection 3.2, we also showed that the

optimization problems consist finally in determining the constant λ_{10} for Case study 1 and constants λ_{10} and λ_{20} for Case study 2 with a "root finding algorithm". However, these strategies are not causal and cannot be applicable for real-world applications. Therefore, an adaptation of these strategies for online implementation is necessary. Over the years, a great deal of efforts has been investigated to cope with online strategies based on non-causal optimal ones [6]. The crucial point of this problem is to find out an appropriate way to adapt the co-state(s) in such a manner that the behavior of causal strategies is as close as possible to the corresponding optimal solution. For simplicity and for computation efficiency, the so-called "λ-control" method is adopted in this work [24,25,10]. This method is based on a feedback control which is easy to implement, see Figure 11. The expression of the estimated $\tilde{\lambda}$ is given as:

$$\tilde{\lambda} = \lambda_0 + K_p\left(SOC_{sp} - SOC\right) + K_i\int_0^t\left(SOC_{sp} - SOC\right) \tag{47}$$

where SOC_{sp} is the SOC set point of the considered energy system storage. This value is given as $SOC_{sp} = SOC(0)$ if the charge sustaining condition is considered. K_p, K_i are the gains of the PI controller and λ_0 is the initial guess.

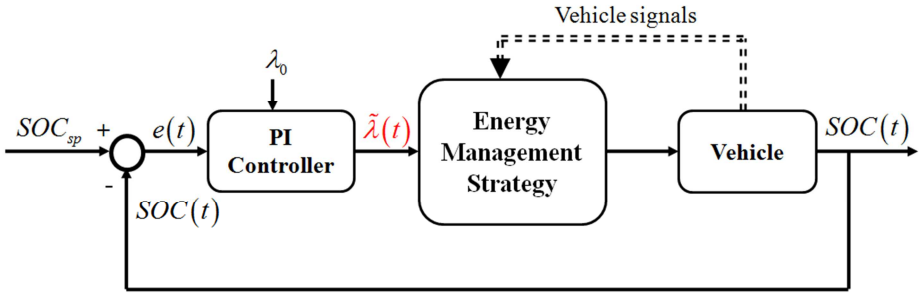

Figure 11. Online estimation of the co-state $\tilde{\lambda}$

It can be noticed that the idea of the "λ-control" method is simply to keep the *SOC* of each energy storage system in a reference range of variation defined by SOC_{sp}. In other words, the feedback "λ-control" aims at preventing the overcharge or depletion of the considered ESS in long

term, however, its SOC may "freely" vary in short term. For this reason, the PI controller gains should be selected rather low. A detail on this discussion can be found in [25].

4.3. Simulation Results

In this work, the Artemis Road cycle [26] will be exclusively considered to validate the different energy management strategies. This driving cycle represents real driving conditions and allows achieving a realistic evaluation of the obtained results. The vehicle speed and gear position of this real-world driving cycle are shown in Figure 12. For all simulations presented hereafter, the tracking performance of the vehicle with respect to the speed reference of the considered driving cycle is always perfectly guaranteed.

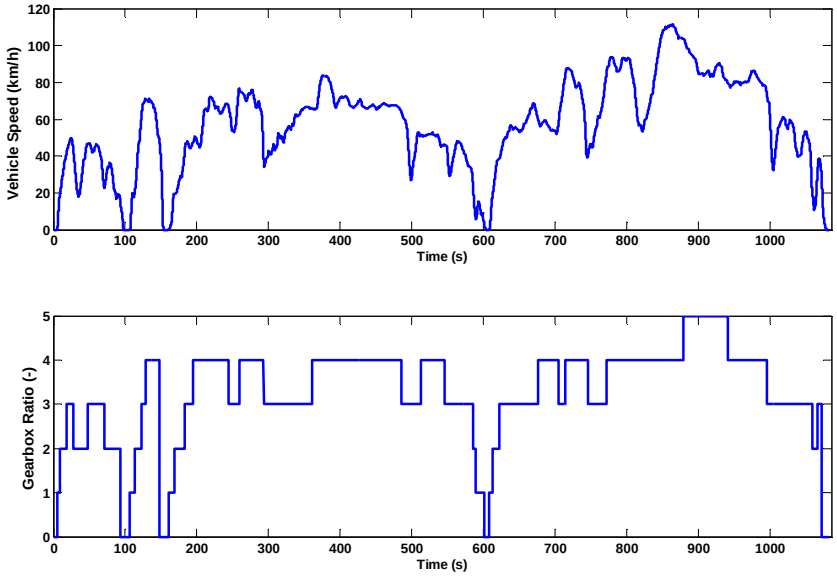

Figure 12. Artemis Road cycle: vehicle speed (up) and imposed gearbox ratio (bottom)

4.3.1. Case study 1

The following strategies are implemented and their results will be compared:

- BL1: Baseline strategy for Case study 1 where the battery is not practically used, so the alternator power is almost equal to the required electric load.
- PMP1: PMP-based optimal strategy for Case study 1 with a given driving cycle.
- RT1: Real-time strategy for Case study 1 with $\tilde{\lambda}_1$ estimated by (47).

The desired and the realized alternator torques obtained from PMP1 strategy are presented in Figure 13. It can be noticed that the alternator toque, which is indirectly imposed by the voltage reference of the electric power system, globally tracks the optimal alternator torque provided by the PMP1 strategy. However, the alternator has its own dynamics. Hence, the realized torque tends to 0 after a certain time for each alternator activation. This problem, which is unavoidable, will degrade the fuel saving performance of the PMP1 strategy. Indeed, the alternator can take some electric energy which is unscheduled by PMP1 strategy.

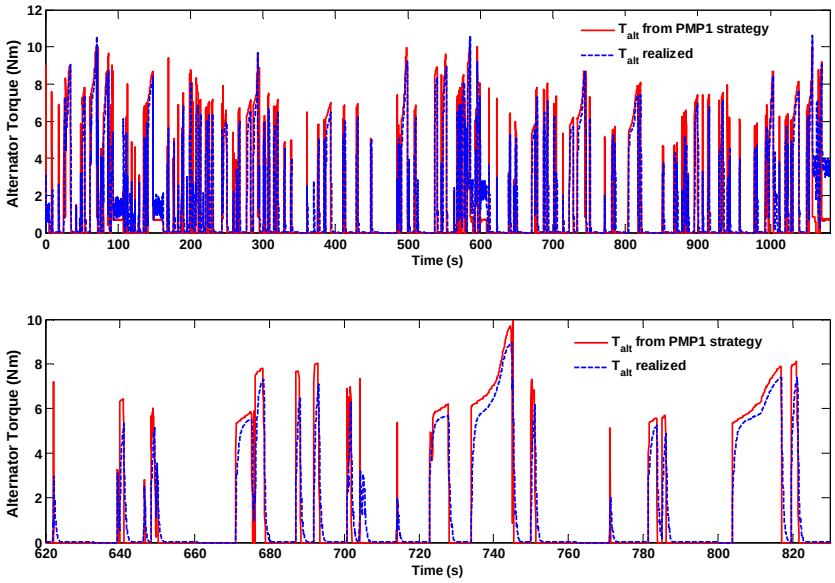

Figure 13. Optimal alternator toque provided by PMP1 strategy and real alternator provided by simulator for all the driving cycle (up) and their zooms (bottom)

Figure 14 shows the comparison of realized alternator torques between PMP1 and BL1 strategies. As previously stated, BL1 tries to maintain a constant alternator voltage; such that the battery is practically not used and all onboard electric load energy is directly supplied by the alternator. Hence, the alternator will be always activated for this strategy and this can increase the fuel consumption. Concerning PMP1 strategy, it schedules the alternator activation at appropriate moments (deceleration phases, battery charging) and with appropriate quantities of torque. In such a manner, PMP1 strategy can help to recover a certain amount of "free energy" coming from regenerative braking. In addition, with this optimal strategy, the alternator can be also used to shift the operating

point of the ICE to other regions that require relative less fuel. Moreover, the battery will be better exploited as shown in Figure 15.

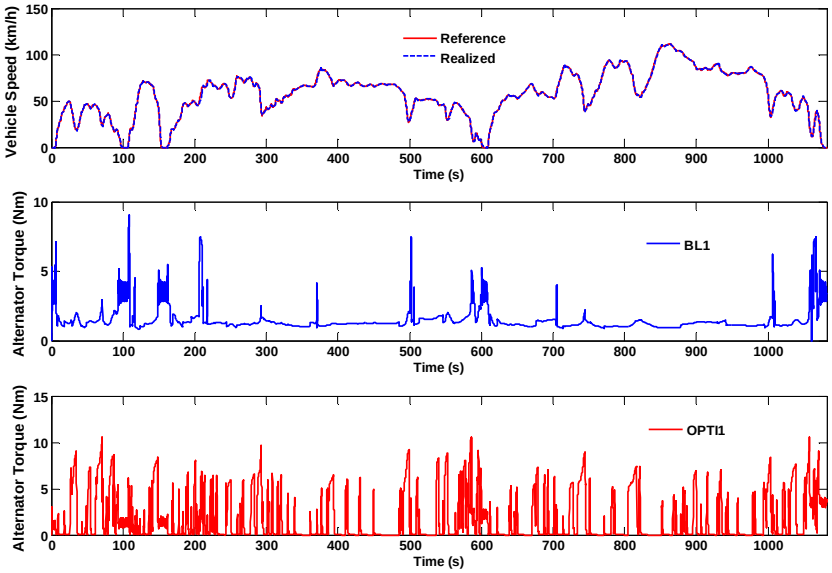

Figure 14. Comparison of realized alternator torques between BL1 and PMP1 strategies

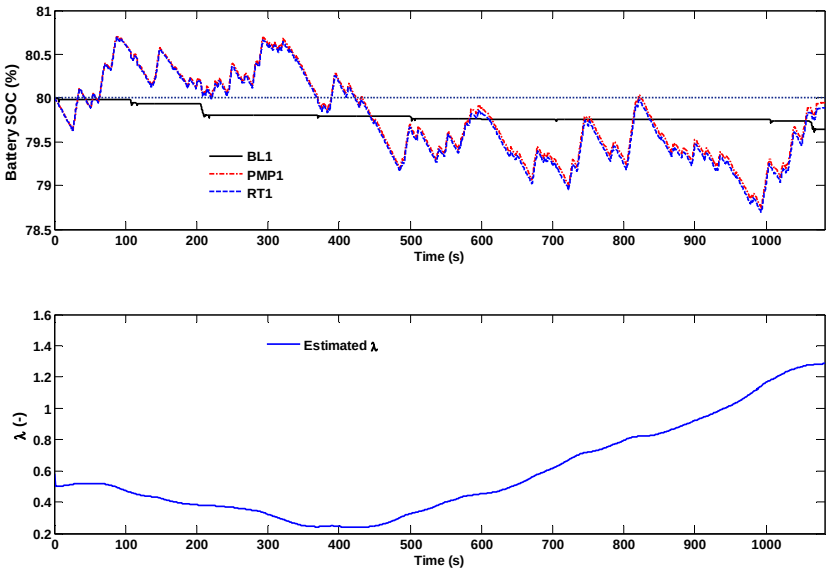

Figure 15. Battery state of charge for different strategies (up); trajectory of estimated $\tilde{\lambda}_1$ corresponding to RT1 strategy (bottom)

From Figure 15, it can be observed that if the co-state $\tilde{\lambda}_1$ is fine tuned then RT1 strategy has the same behaviors as PMP1 strategy although it does not need any information on the future of driving cycle. Table 1 summarizes the energy consumption of the considered strategies and the fuel saving of PMP1

484 and RT1 strategies with respect to BL1 strategy for Artemis Road cycle. This table shows that the
485 proposed strategies (OPTI1 and RT1) are not only effective to reduce the fuel consumption but also
486 can guarantee the sustaining charge condition of the battery.

Strategy	Fuel Use [g]	Fuel Saving [%]	ΔSOC_{bat} [%]
BL1	700.072	0	0.361
OPTI1	685. 597	2.068	0.056
RT1	685.776	2.042	0.111

487 Table 1. Summary of energy consumption for different strategies of Case study 1

488 *4.3.2. Case study 2*

489 As previously stated, searching offline optimal solution with "root finding algorithm" can be too
490 expensive in terms of simulation time. Hence, this will be not presented here and only two strategies
491 are implemented and compared in this case:

492 • BL2: Baseline strategy for Case study 2 uses only the supercapacitor. The DC/DC converter
493 is controlled by a heuristic strategy of industrial partner. This strategy aims at guaranteeing
494 that the voltage in the supercapacitor side is always superior to the one in the battery side and
495 the supercapacitor energy is always kept between certain levels.

496 • RT2: Real-time strategy for Case study 2 with $\tilde{\lambda}_1$ and $\tilde{\lambda}_2$ estimated by (47).

497 The results of BL2 and RT2 strategies are compared in Figure 16. The same comments on the
498 alternator activation can be done as in Case study 1, i.e. the alternator is mostly activated by RT2
499 strategy to recover regenerative braking energy. Moreover, RT2 strategy also activates the DC/DC
500 converter more often than BL2 strategy to charge the supercapacitor at appropriate moments. As a
501 consequent, both energy storage systems (ESS) are better exploited in RT2 strategy than in BL2
502 strategy as shown in Figure 17.

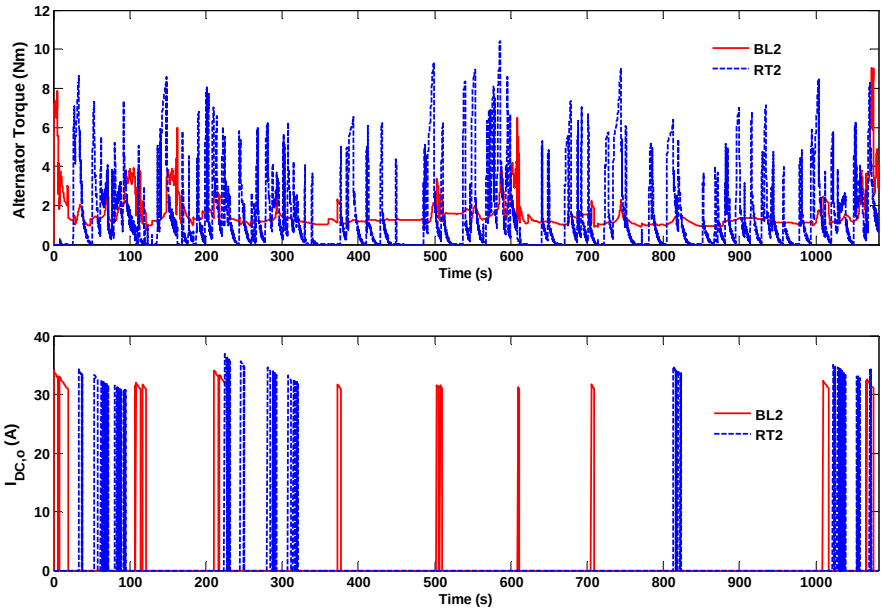

Figure 16. Comparison of alternator torque and converter current between BL2 and RT2 strategies

It can be also observed from Figure 17 that the charge sustaining conditions for both ESSs are guaranteed by RT2 strategy whereas BL2 strategy cannot fulfill this condition for the supercapacitor. Indeed, BL2 strategy only has tendency to charge the supercapacitor. Moreover, as previously stated, the use of the battery is very limited in this case; in particularly the battery SOC with BL2 strategy is almost constant for the entire driving cycle.

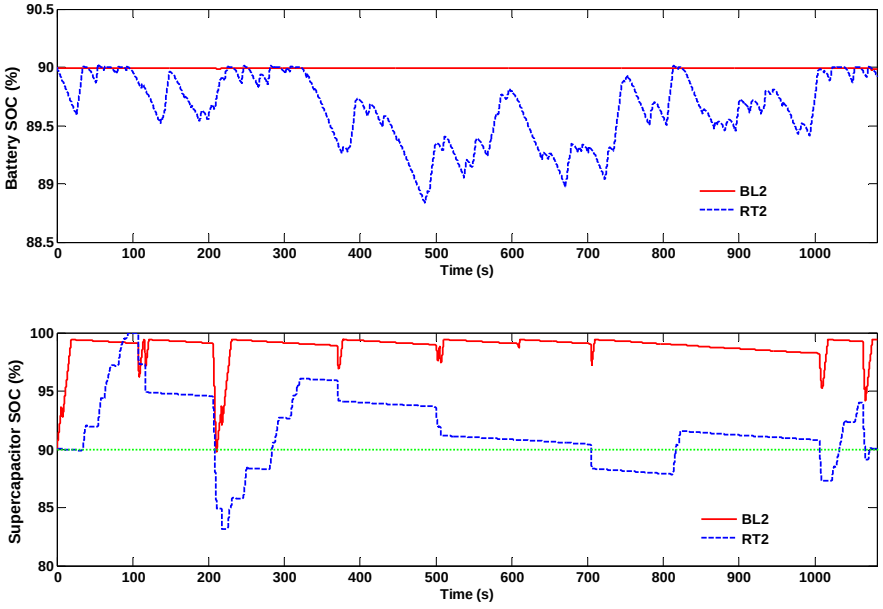

Figure 17. Comparison of ESS state of charges between BL2 and RT2 strategies

Figure 18 shows that supercapacitor voltage always remains in its operating range, i.e. it is always higher than the battery voltage as imposed by the electric power system and lower than the supercapacitor voltage maximal value (16.2V). Thanks to the penalty function $\lambda_d \dot{X}_d = \lambda_{d0} \dot{X}_d$ incorporated into the Hamiltonian, the supercapacitor voltage only touches its upper limit for a very short time (around 100s) of the driving cycle.

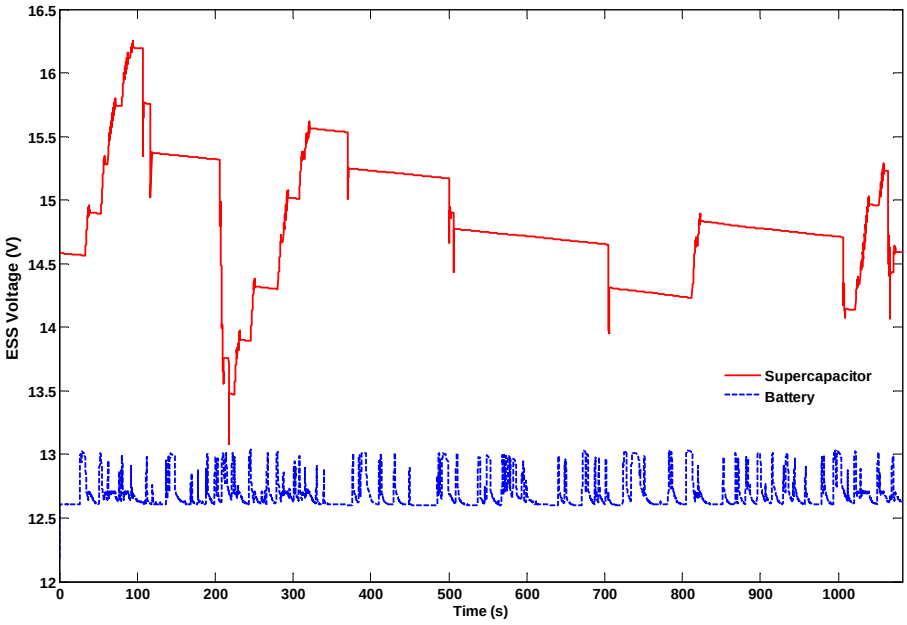

Figure 18. Voltages of energy storage systems for RT2 strategy

Table 2 summarizes the energy consumption of both strategies, and the fuel saving of RT2 strategy with respect to BL2 strategy for Artemis Road cycle. From the results, it can be concluded that the RT2 strategy is effective for fuel consumption reduction.

Strategy	Fuel Use [g]	Fuel Saving [%]	ΔSOC_{bat} [%]	ΔSOC_{sc} [%]
BL2	701.819	0	0.019	9.394
RT2	690.322	1.634	0.076	0.054

Table 2. Summary of energy consumption for different strategies of Case study 2

As can be seen, the results obtained on this unique cycle are very promising. However, several tests with other driving cycles would be necessary to show that the extra energy consumption of eSC

would be compensated with some effective energy management strategies (note that the eSC is practically only activated in low load region).

5. Concluding Remarks

In this work, PMP-based strategies are developed to "optimally" control the vehicular electric power systems. We have shown that this approach has several advantages for real-time implementation. First, causal strategies, which can mimic the behavior of optimal solution, can be easily obtained with a simple feedback control scheme. Second, it is very efficient in terms of time computation because it is based on the instantaneous minimization of the Hamiltonian. The effectiveness of the approach is pointed out through several simulation results for both case studies. Most of fuel saving comes from regenerative braking which is "free" energy. Despite the additional cost for hardware investments, the dual storage electric power system offers a limited fuel saving performance compared to single storage electric power system for the given parameter values in the simulator AMESim. However, this electric structure may be used to reduce the capacity of the battery since it is not practically used or it would be more interesting for electric hybrid vehicles with "stop and start" operation.

The energy management problem considered in this work can be directly applied to parallel hybrid electric vehicles. They are also easily generalized to others hybrid architectures with some slight modifications.

Acknowledgements

This research is sponsored by the International Campus on Safety and Intermodality in Transportation the Nord-Pas-de-Calais Region, the European Community, the Regional Delegation for Research and Technology, the Ministry of Higher Education and Research, and the French National Center for Scientific Research. This work is also sponsored by the FUI and VALEO Group through the SURAL'HY project.

549 **References**

550

[1] W. Soong, N. Ertugrul, E. Lovelace, and T. Jahns, "Investigation of Interior Permanent Magnet Offset-Coupled Automotive Integrated Starter/Alternator," in *Industry Applications Conference*, Chicago, IL, USA, 2001, pp. 429-436.

[2] A. Khaligh and Li Zhihao, "Battery, Ultracapacitor, Fuel Cell, and Hybrid Energy Storage Systems for Electric, Hybrid Electric, Fuel Cell, and Plug-In Hybrid Electric Vehicles: State of the Art," *IEEE Transactions on Vehicular Technology*, vol. 59, no. 6, pp. 2806-2814, 2010.

[3] K. Çağatay Bayindir, M.A. Gözüküçük, and A. Teke, "A Comprehensive Overview of Hybrid Electric Vehicle: Powertrain Configurations, Powertrain Control Techniques and Electronic Control Units," *Energy Conversion and Management*, vol. 52, no. 2, pp. 1305-1313, 2011.

[4] R.E. Bellman, *Dynamic Programming*. Princeton, USA: Princeton University Press, 1957.

[5] L.S. Pontryagin, V.G. Boltyanskii, R.V. Gamkrelidze, and E.F. Mishchenko, *The Mathematical Theory of Optimal Processes*. New York: Interscience Publishers, 1962.

[6] A Sciarretta and L. Guzzella, "Control of Hybrid Electric Vehicles: a Survey of Optimal Energy Management Strategies," *IEEE Control Systems Magazine*, vol. 27, no. 2, pp. 60-70, 2007.

[7] O. Sundström, "Optimal Control and Design of Hybrid Electric Vehicles," ETH Zurich, PhD Thesis 2009.

[8] C.C. Lin, H. Peng, J.W. Grizzle, and J.M. Kang, "Power Management Strategy for a Parallel Hybrid Electric Truck," *IEEE Transactions on Control Systems Technology*, vol. 1, no. 6, pp. 839-849, 2003.

[9] M. Koot et al., "Energy Management Strategies for Vehicular Electric Power Systems," *IEEE Transactions on Vehicular Technology*, vol. 54, no. 3, pp. 771-782, 2005.

[10] T.J.B.A. Kessels, "Energy Management for Automotive Power Nets," Technische Universiteit Eindhoven, PhD Thesis 2007.

[11] S. Delprat, J. Lauber, T.M. Guerra, and J. Rimaux, "Control of a Parallel Hybrid Powewtrain: Optimal Control," *IEEE Transactions on Vehicular Technology*, vol. 53, no. 3, pp. 872-881,

2004.

[12] A. Ambühl, O. Sundström, A. Sciarretta, and L. Guzzella, "Explicit Optimal Control Policy and Its Practical Application for Hybrid Electric Powertrains," *Control Engineering Practice*, vol. 18, no. 12, pp. 1429-1439, 2010.

[13] G. Paganelli, T.M. Guerra, S. Delprat, Y. Guezennec, and G. Rizzoni, "Optimal Control Theory Applied to Hybrid Fuel Cell Powered Vehicle," in *15th IFAC World Congress*, Barcelona, 2002, pp. 1508-1508.

[14] A. Sciarretta, M. Back, and L. Guzzella, "Optimal Control of Parallel Hybrid Electric Vehicles," *IEEE Transactions on Control Systems Technology*, vol. 12, no. 3, pp. 352-363, 2004.

[15] V. Paladini, T. Donateo, A. de Risi, and D. Laforgia, "Super-capacitors Fuel-cell Hybrid Electric Vehicle Optimization and Control Strategy Development," *Energy Conversion and Management*, vol. 48, no. 11, pp. 3001-3008, 2007.

[16] A. Poursamad and M. Montazeri, "Design of Genetic Fuzzy Control Strategy for Parallel Hybrid Electric Vehicles," *Control Engineering Practice*, vol. 16, no. 7, pp. 861-887, 2008.

[17] M.A. Hannan, F.A. Azidin, and A. Mohamed, "Multi-sources Model and Control Algorithm of an Energy Management System for Light Electric Vehicles," *Energy Conversion and Management*, vol. 62, pp. 123-130, 2012.

[18] P. Sharma and T.S. Bhatti, "A Review on Electrochemical Double-layer Capacitors," *Energy Conversion and Management*, vol. 51, no. 12, pp. 2901-2912, 2010.

[19] S. Fiorenti, J. Guanettia, Y. Guezenneca, and S. Onori, "Modeling and Experimental Validation of a Hybridized Energy Storage System for Automotive Applications," *Journal of Power Sources*, vol. 241, pp. 112-120, 2013.

[20] J. Heywood, *Internal Combustion Engine Fundamentals*.: McGraw-Hill, Inc, 1988.

[21] N. Kim, S. Cha, and H. Peng, "Optimal Control of Hybrid Electric Vehicles Based on Pontryagin's Minimum Principle," *IEEE Transactions on Control Systems Technology*, vol. 19, no. 5, pp. 1279-1287, 2011.

[22] D.E. Kirk, *Optimal Control Theory: An Introduction*.: Englewood Cliffs : Prentice-Hall, 1970.

[23] W. Borutzky, *Bond Graph Methodology: Development and Analysis of Multidisciplinary Dynamic System Models*.: Springer, 2010.

[24] S Delprat, T.M. Guerra, and J. Rimaux, "Optimal Control of a Parallel Powertrain: from Global Optimization to Real Time Control Strategy," in *IEEE Vehicular Transportation Systems*, Atlantic City, USA, 2002, pp. 2082-2088.

[25] M.W.T. Koot, "Energy Management for Vehicular Electric Power Systems," Technische Universiteit Eindhoven, PhD Thesis 2006.

[26] M. André, "The ARTEMIS European Driving Cycles for Measuring car Pollutant Emissions," *Science of The Total Environment*, vol. 334-335, pp. 73-84, 2004.

551

552 **Appendix.** Some notations of vehicle variables used in this paper

Variable	Description	Unit	Variable	Description	Unit
T_w	Wheel torque	Nm	ω_w	Wheel speed	rpm
T_{ice}	ICE torque	Nm	ω_{ice}	ICE speed	rpm
T_{alt}	Alternator torque	Nm	ω_{alt}	Alternator speed	rpm
T_{ps}	Primary shaft torque	Nm	ρ	Gear ratio of the reducer	--
η_{gb}	Gearbox efficiency	--	k	k^h gear of the gearbox	--
Q_{lhv}	Constant fuel energy density	kJ/kg	$R(k)$	Gearbox ratio of the k^{th} gear	--

553